International Research Journal of Earth Sciences ISSN 2321–2527
Vol. **1(3),** 1-10, June **(2013)** *Int. Res. Earth Sci.*

Shear – Lineaments Analysis of Ambasamudram-Tenkasi Transect of Achankovil – Tambraparani Shear Zone, South India

Manimaran G.[1] P.T. Roy Chacko[2], Manimaran D.[1], Selvam S.[1], A. Antony Ravindran[1], Besheliya J.[1] and Sugan M.[1]
[1]School of Tectonics, Department of Geology, V.O.Chidambaram College, Thoothukudi-628008, INDIA
[2]Chandrakantham, Thundathil, Khazhakuttom, Kerala-695582, INDIA

Available online at: www.isca.in
Received 27th May 2013, revised 10th June 2013, accepted 22nd June 2013

Abstract

Remote sensing and field studies of Ambasamudram – Tenkasi transect a part of Achankovil-Tambraparni Shear Zone of south India reveal five different pattern of lineaments i.e. (i) ENE –WSW to E – W (ii) NNW – SSE to NW – SE (iii) NNE – SSW to NE –SW (iv) NW – SE to WNW – ESE and (v) N – S. Based on shear sense and field association nine prominent shear-lineaments related to D1, D2, D3 and D4 deformation have been delineated. Mean frequency, mean density and nearest neighbor analysis of shear- lineaments form a tool to distinguish the intensity of deformation and to predict the order of decreasing intensity of deformation i.e. D3, D2, D4 and D1. The random and regular patterns of individual shear-lineaments were observed and their restriction to a specific lithology and geomorphic expression are pointing towards a genetic link between them.

Keywords: Shear-lineaments, Achankovil-Tambraparni Shear, deformation, nearest neighbor analysis, LANDSAT image, South India

Introduction

The earlier works on lineaments have noticed that the intense deformations are often localized in narrow sub-parallel sided zones which are loosely termed shear zones[1-3]. Such shear zones vary in size from hundreds of kilometers[4] through an outcrop scale[5] to a microscopic scale[6]. The Riedel shear structure, first reported by Cloos H. and Riedel W.[7,8]. In clay-cake experiments, was realized to be fundamental structure in shear zones. The basic geometry of the Riedel structure consists of conjugate shear bands arranged in en-echelon arrays and denoted by R and R'. The R- bands are synthetic to the sense of slip across the shear zone forming right-stepping en-echelon arrays along shear zones and left-stepping arrays along dextral shear zones. The R' bands are antithetic and usually connect overlapping R-bands[8,9]. Lineaments are natural, linear surface elements interpreted directly from satellite imagery and geophysical map as fracture traces used for water resource management[10] and structural geologic studies[11,12]. Right overstepping linements, sinistral shear bands suggest sinistral transpressive deformation of Achankovil shear zone was reported[13]. From the three-dimensional finite strain patterns, sinistral transpressive nature of Achankovil shear zone, South India was inferred[14]. Vallanadu area is a high grade metamorphic terrain of amphibolite to granulite grade forms a part of Achankovil shear zone and had experienced dextral and sinistral shears of conjugate fracturing nature was delineated[15]. From the analysis of lineament swarms from Balarampur area of West Bengal[16] it is concluded that the tectonic strain and fracture frequency play vital role in the generation of lineaments in the older metamorphic terrains.

Study area: The Achankovil-Tambraparni Shear zone (ATS) is a well deciphered lineament of 8-25 km width on LANDSAT imageries and aerial photo mosaic trending WNW-ESE to NW–SE direction. It extends from the southwestern (N 09°20’00”; E 76°30’00”) to the southeastern (N 08°20’00”; E 78°10’00”) coasts of India (length 210 km). Southwestern border of ATS zone, another contiguous, parallel shear zone, Tenmalai-Gatana shear (TGS) was reported[17-20]. Lineaments, faults and shears of megascopic to microscopic dimensions are very well developed within the charnockite- khondalite complex of Ambasamudram - Tenkasi transect of ATS-TGS zones.

Material and Methods

The complex pattern of lineaments of different orientations, genetic sequence and times were studied through remote sensing, field mapping (1:25,000 scales) and lithological studies. The order of intensity of deformations was determined with the help of statistical analysis using nearest neighbor analysis.The study area lies across ATS and TGS zones and between E8°45' and E9°00' and N77°15'and N77°30'. Amphibolite facies to granulite facies high grade metamorphic rocks are exposed in this area.

The pattern of lineaments and their associated lithology and geomorphology were studied using stereo pairs of 1:25,000 scale for cloud free black and white aerial photographs (Task No.1015-A Run Nos./photo Nos. 45/9-15, 46/1-10, 47/1-6, 49/1-6,50/1-3,53/9-16,56/7-14, 61/4-8 and 63/7-12) at Institute of Remote sensing, Anna University, Madras. Using the photo

characteristics structural, physiographic and lithological features were identified from the imageries and further correlated and supplemented by field observations.

Results and Discussion

Remote sensing studies: Two broad lithounits were identified from the aerial photographs on the basis of tonal differences viz. i. Khondalite ii. Charnockite belts. The southern khondalite belt composed of garnetiferous biotite sillimanite gneiss with intercalation of quartzites, cordierite gneiss and highly deformed calc-silicate rocks are traced by their dark tones and banded appearance, whereas the northern granulites (charnockites) were identified by their characteristic medium to dark grey tones and massive appearance. Apart from these two lithotypes, a linear belt of grayish-white tone is also observed in the zone of khondalite and charnockite and from the field checks the linear belts were identified as granitised migmatite complexes of khondalites and charnockites. Apart from the northern massive charnockite belt another massive charnockite band running through Ambasamudram and Sivasailam and a folded massive charnockite unit, north of Kadayam were observed within the southern khondalite belt (figure 1) Geomorphic Expressions of Lineaments.

Based on the geomorphic expressions, the area is classified into two units viz. 1, Highland (HL, >150m above MSL) which is characterized by the ridges and valleys of mountainous terrain and 2, Lowland (LL, <150m) characterized by low mount ridges and plains with a rolling topography. The high and lowlands occur in the western and eastern parts of the study area respectively (figure 1). The drainage patterns also confirm this classification: the highland has a higher drainage density than the lowlands (figure 2) irrespective of lithology of the area. Freely developed dendritic and structurally controlled rectangular and trellis patterns of drainage are observed in low and highlands. A detailed field checks of the area helped to bring out a series of fault scarps (step faults) at west of Kadaiyam and Kuttalam and Palayakuttalam; upward thrusting of lithounits along ATS zone and rhomb-shaped depressions along step faults of TGS zone, suggest different style of imbrication structure.

All along the highland, a triangular rugged profile is common where two or three set of fault scarps meet at a point (figure 2). The above features are not seen in the lowland (except a few fault scarps on the low mounts) owing to high degree of denudation and the resultant peneplanation. Since the geomorphic expression of the lineaments varied on elevation and lithology, it was decided to analyze the linear features of highland and lowland and charnockite and gneissic khondalite terrains separately and synoptically.

Shear sense and chronological order of lineaments: An analysis of the orientation of the study area reveals five distinct sets of lineaments trending; i. ENE-WSW to E-W, ii. NNW-SSE to NW-SE, iii. NNE-SSW to NE-SW, iv. NW-SE to WNW-ESE and v. N-S. The lineaments of the study area are classified into three units on the basis of their length (l in km) as i. Major lineaments (l>=10), ii. Meso lineaments (10<l>1) and iii. Micro lineaments (l<=1). The micro lineaments were identified in the field while the major and meso lineaments were delineated on aerial photographs; topographical and geological maps of different scales. The attitude of the micro lineaments (i.e. shear, faults, boudinage zones, sheared axial planes and trends of emplacements), the associated shear sense and type of shear zones were recorded in the field. Attitudes and up throw side of the major and meso fault scarps were observed during the field check of the aerial photo data.

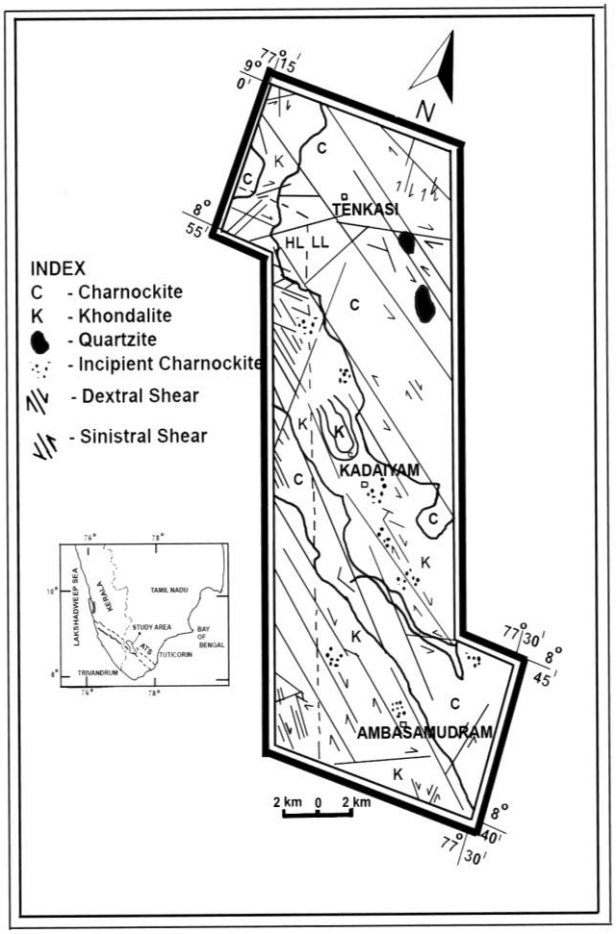

Figure-1
Shear-lineaments map of Ambasamudram-Tenkasi transect of Achankovil –Tambraparani shear and Tenmalai-Gatana shear zones

Kinematics and genesis of different types of coaxial and non-coaxial deformations has been a subject of discussion for a number of years[1,8,21-27]. Nearly 400 micro shear zones (length <=1km) of various types were mapped in detail in 1:25,000 scale. Most observations made on either horizontal planes or vertical sections made it possible to reconstruct the shape and orientations. Interestingly concordance between the strike of the larger lineaments observed during the remote sensing studies

and that of the micro lineaments were established during the field studies. Since most of the shears are propagated along the veins and bands of pegmatite, the dilatation or displacement of veins by later shears are very common features in ATS and TGS zones.

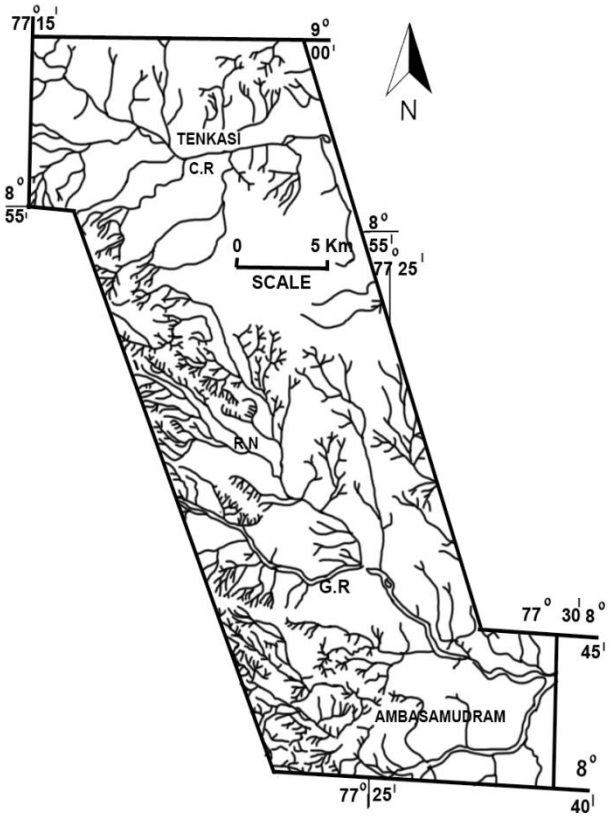

Figure.2
Drainage density pattern from Ambasamudram-Tenkasi area, T.R- Tambraparani river, G.R-Gatana river, C.R-Chittar river and R.N-Rama Nadi

In a strike-slip regime, two principal types of mechanisms explain the geometric and dynamic relations among the shears and associated structures viz. 1, Pure shear (coulomb-Anderson model)[21] and 2, Simple or "direct"shear. Pure shear produces relatively short, typically conjugate sets of strike-slip faults which help to accommodate the brittle component of strain in tectonic regimes of crustal shortening. Bulk shear is irrotational and has an orthorhombic symmetry where as simple shear has a monoclinic symmetry and rotational component of bulk strain and accounts for the kinematics of strike-slip faults at all dimension[24].

In the case of strike-slip regime, pure shear shows a conjugate set of complementary sinistral and dextral strike-slip faults will form at an angle of ϕ and $-\phi$ about the shortening direction, where ϕ is the angle of internal friction. The extension fractures or normal faults will form perpendicular to elongation axis and those folds and thrust faults will form perpendicular to the shortening axis[28].

The simple shear produces a greater variety of structures other than the pure shear. The experimental deformation of homogeneous rocks under confining pressure generates five sets of fractures form in simple shear like: i. Riedel (R) shears or synthetic shear[24], ii. Conjugate Riedel (R') shears[24] "antithetic" shears, iii. Secondary synthetic strike-slip faults at an angle of $-\phi/2$ to the direction of applied shear (P shears)[22,24], iv. Extension fractures (T fractures)[25] or normal faults which develop at about 45° to the principal displacement zone (PDZ) and v. Faults parallel to the principal displacement zone (PDZ) Y shears[23].

The sense of strike-slip along the R, P and Y shears is the same as that of the basement fault (PDZ) where as that of the R' it is in the opposite direction. The R and R' shears make angles of $\phi/2$ and $(90°-\phi/2)$ (where ϕ is the angle of internal friction) respectively with the principal displacement zone (PDZ)[28]. The strike of R shears[25] deflect 15° to 20° to the principal displacement zone and that of R' shears form 60° to 75°. The extension fractures bisect the angle between the R and R' shears and are oriented parallel to the incremental axis of shortening and at an angle of 45° to the direction of applied shear. R' shears are rarely developed in the nature except where there is a substantial overlap between adjacent R shears[29]. The P shears are formed as a consequence of the reduction of shearing resistance along the R shear [24]. Reorientation of shortening axis towards the R shear produce P shear in a local strain field that strike at an angle of $-\phi/2$ to the PDZ[29]. Folds and thrust faults form initially perpendicular to the axis of shortening viz. at an angle of 45° to the PDZ. If deformation continues, then the fold axes will rotate according to amount of shearing as much as 19° for a shear strain of unity[30].

One of the striking features of the angular relationship between the conjugate sets of ductile shears unlike the brittle shear zones[21], is that it is the obtuse angle (generally 90° to 130°) between the shears which faces the greatest shortening direction ($\sigma 1$) of the system[1] and the minimum compression direction ($\sigma 3$) is given by the acute bisector and the zone of intersection parallels the intermediate compression direction[3] ($\sigma 2$), showed that though the shear zone rotates during a progressive deformation, the direction of bulk shortening (obtuse bisector) and bulk stretching (acute bisector) maintain nearly constant orientations.

In the light of above discussion, chronologically the lineaments formed due to consecutive shearing of the area[31] are, i. Lineaments/Shears of D1 deformation, L1 - ENE-WSW dextral brittle shear (rarely preserved) (figure-3).

Lineaments/Shears of D2 deformation: L2 – NW-SE (Tenmalai – Gatana shear-PDZ) to NNW – SSE (L2R riedel shear) dextral, brittle-ductile shears (figure 4).

L2R'- NNE-SSW to NE-SW sinistral, brittle-ductile conjugate riedel shear (figure 5)

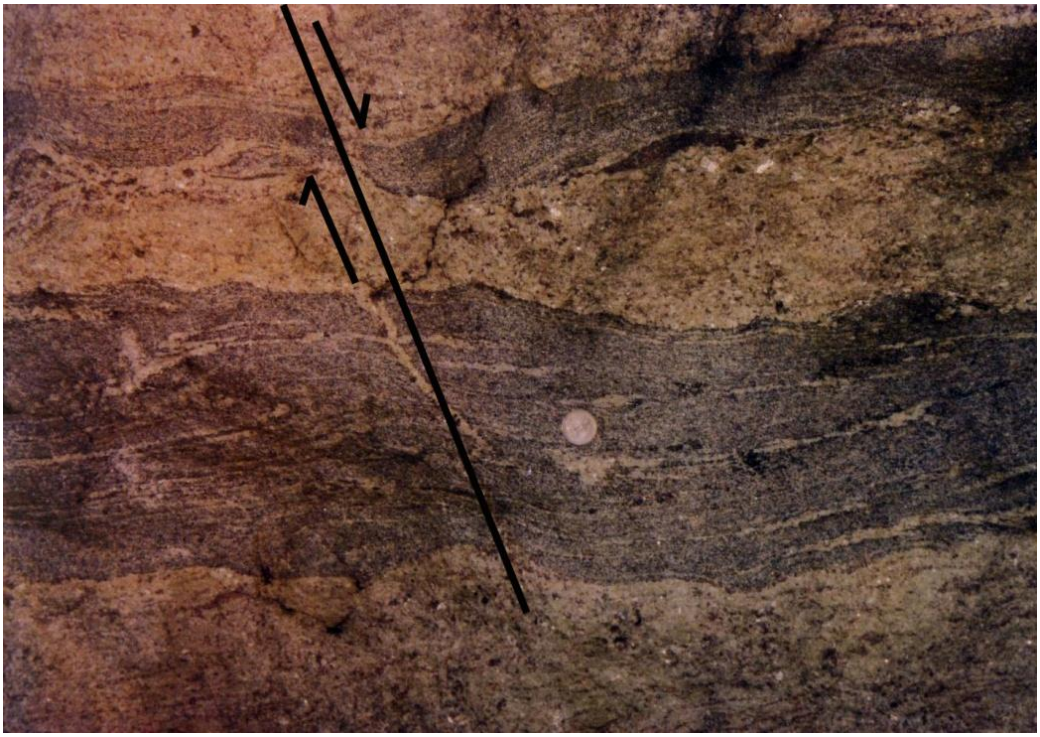

Figure-3
Relict patches of biotite gneiss within the later granitic gneiss (formed during L2; Tenmalai Gatana Shear) showing a dextral brittle L1 shear (N70°E 65°NW near the coin) (Location – Ambasamudram)
L1C – N-S sinistral as a conjugate brittle micro shear or fracture

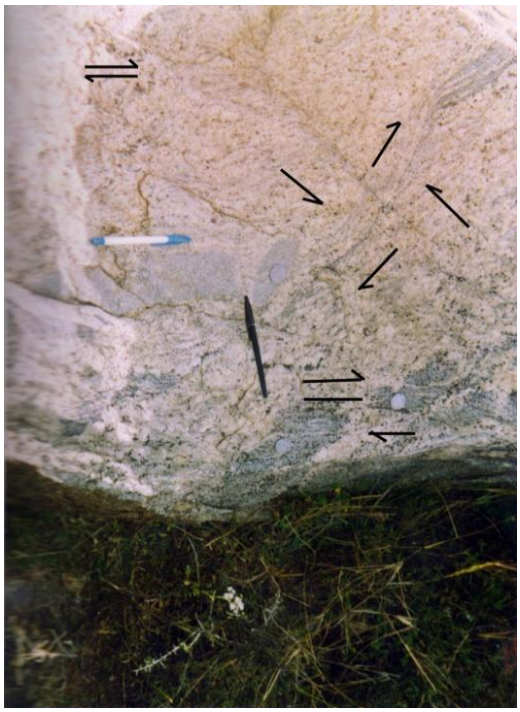

Figure-4
Granitic gneiss showing dextral bulk shear and a rotated lense garnet biotite gneiss between NW-SE dextral TGS (white pen) and NE-SW sinistral shear (black pen) of D2 deformation dextrally displaced biotite rich band (two pen) are also seenat the bottom. Approximately E-W sinistral L3R conjugating with N-S dextral shear of L3R' are also developed at right middle of the exposure (Location-Ambasamudram)

Lineaments/Shears of D3 deformation: L3 - NW-SE to WNW-ESE (Achankovil – Tambraparani shear-PDZ) sinistral, ductile-brittle shear (figure 6). L3R- E-W (P shear) to WNW-ESE sinistral, ductile, brittle riedel shear. L3R'- N-S dextral, brittle-ductile conjucate riedel shear (figure 7).

Figure-5
From TGS zone, near Ambasamudram Granitic gneiss shows a series of NE-SW sinistral Riedel shear bands of L2 (seen oblique to the pens). Along and across the shear bands granitic gneiss are converted into incipient charnockite due to D2 (L2) deformation and infiltration of Co2 gas along the shears and dehydration related charnockitisation

Figure-6
Foliations of Cordierite gneiss and pegmatite showing sinistral shearing along a NW-SW ductile shear ATS-L3 at Valliammalpuram NE of Kadayam from Achankovil shear zone

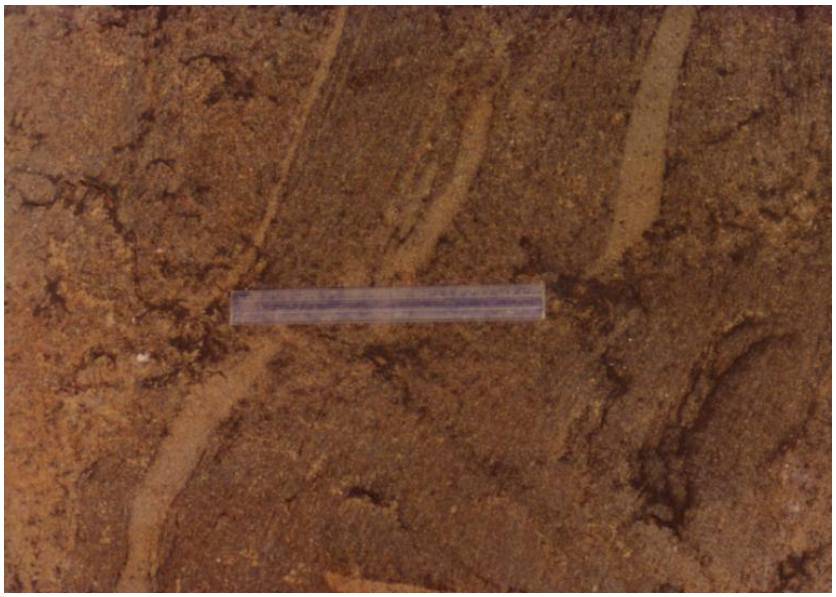

Figure-7
A retrograded gneiss showing N-S dextral shear near Tenkasi, complementary Riedel shear of major Achankovil-Tambraparni shear. Note the displacements in grey granite veins (Location-Sengottai)

Table - 1
Linear density and frequency distribution of shear-lineaments of different deformations from the study area. λ-Linear density; F-Frequency; L-Length of lineaments in km; Σ1-total lengths in km; OF-Overall frequency; Sh-Shear; Major > 10 km; Meso 10<l>1 km and Micro l<1 km. Values in the parantheses represent the reactivated lengths

Deformation D	Sh.Lineaments L	TGS			ATS			Total Area			
		Major (l) km	Meso (l) km	Micro (l) km	Major (l) km	Meso (l) km	Micro (l) km	Total l Σ	LD λ	F	OF
D1	L1	Nil	12.063	0.430	Nil	3.50	0.060	16.053	0.028	0.0 0.2 0.6	0.27
D2	L2	100.125 (32.375)	44.19 (15.38)	5.75 (0.15)	Nil	24.69 (5.0)	9.14 (1.47)	183.9	0.315	0.0 0.2 2.8	1.0
	L2R'	Nil	14.94	1.37 (0.2)	Nil	20.44	1.30 (0.07)	38.05	0.07	0.0 0.2 1.0	0.40
D3	L3	32.38	29.06	1.98	82.0	63.44	14.27	223.14	0.38	0.2 0.8 3.2	1.4
	L3R	Nil	12.50	0.26	Nil	9.627	2.65 (0.06)	25.03	0.043	0.0 0.2 0.8	0.33
	L3R’	Nil	3.25	0.85	Nil	14.12	2.38	26.60	0.04	0.0 0.2 0.8	0.33
	L3T	Nil	Nil	0.26	Nil	19.75	3.56	23.56	0.04	0.0 0.6 1.0	0.53
D4	L4	Nil	15.44	1.2	Nil	18.88	5.81	54.76	0.09	0.0 0.2 0.8	0.33
	L4R’	Nil	5.811	1.583	Nil	28.25	6.775	42.42	0.073	0.0 0.2 1.0	0.40

L3T- ENE-WSW (NE-SE) dextral, brittle tension, shear fracture along the maximum compression direction of D3.

Lineaments/shears of D4 deformation: L4- N-S (Toranamalai shear) to NNW-SSE (L4R riedel shear) sinistral brittle-ductile shear. L4R'- E-W dextral, brittle-ductile conjugate riedel shear (figure 1).

Frequency and Linear distribution of various shear-lineaments: The frequency distribution for each type of lineaments were computed by counting the number of observations (n) of major and meso lineaments of a specific type at a distance (D) measured at right angles to the strike of the lineaments, so that frequency (f) = (n/D). Observations were made for constant D=5 km. Individual frequencies were calculated for different sets. The total lengths (Σl) of the each set of lineaments were computed by summing the observed length of major, meso and also micro lineaments of that set. Linear density λ was computed from Σl/A, where, A is the area of observation. Some of the shear-lineaments were reactivated in an opposite direction during the subsequent deformation and their reactivated lengths (given within parentheses in table no.1) were also taken while computing the linear density of similarly oriented shear-lineaments of subsequent age. For example NW-SE dextral L2 of D2 in all dimensions got reactivated as NW-SE sinistral L3 of D3 age. Similarly NE-SW sinistral micro L2R of D2 got reactivated as NE-SW dextral L3T of D3 and E-W sinistral L3R of D3 as E-W dextral L4R of D4. The table 1 reveals the prominent nine patterns of shear-lineaments one could able to trace in TGS and ATS regimes. The figure 8 graphically represents the λ and $\overline{f}$ (mean frequency) of individual shear lineaments. L3 of D3 has the maximum density (0.382) and L2 of D2 comes next (0.315). L4 of D4 comes third (0.09) and the remaining is not significant.

As per the mean frequency (*f*) data L3 of D3 and L2 of D2 are the most prominent ones (1.4 and 1.0 respectively). L3T of D3 follows them but its density is negligible. This is due to the development of the largest number of L3T shear-lineaments especially in ATS regime. The L4 of D4 though are longer they are lesser in number. Among the different periods of deformations the maximum mean linear density was observed for D3 (0.5) and D2 comes next (0.38). The D4 (0.167) and D1 (0.028) follows in that order. The above order may be taken as a measure of intensity of deformation. The mean frequency distribution *f* of shear –lineaments of different deformations follows the same order of mean density (D3=2.6, D2=1.4, D4=0.73 and D1= 0.266). These observations point out that the features evolved during D3 deformation (ATS) were least affected by the later D4 (TS) and features of D2 were affected by the later D3 and D4 deformations.

Nearest neighbor analysis of shear lineaments: To find out the level of significance (Z test) of each lineament patterns and their indices for spatial distribution (Spatial Index, R) of each lineament, the nearest-neighbor analysis[32] has been carried out for each prominent pattern of lineaments (Shears) of D1, D2, D3 and D4 deformations. By this method, the level of significance of a set of lines is tested with reference to a general pattern generated by random lines. For this analysis only major lineaments (l>10km) and meso lineaments (10<l<1km) of the study area are taken into account.

Pattern of shear-lineaments and their significance: The pattern, influence and extend of expression of the various sets of lineaments of four episodic deformations, were studied using nearest neighbor analysis. The lineament data were grouped on parameters like, i. Deformations (D1, D2, D3 and D4), ii. Shear sense (dextral and sinistral), iii. Size of lineaments – Major and meso (length l in km), iv. Geomorphology (Highland 98 km2 and lowland 486km2), v. Lithology (Khondalite 346 km2 and Charnockite 238 km2) and vi. Major shear regimes (TGS regime 231 km2, ATS regime 353 km2 and total area 584 km2).

Tenmalai-Gatana shear (TGS) regime and Achankovil-Tambraparni shear (ATS) regime seen in areas exposed at SW and NE of Idikal-Kadayam stretch respectively. Since the method uses the relationship between adjoining pair of structural trends only those lineaments that was measured normal to the neighboring lineament were taken into account. If a lineament was observed in khondalite and charnockite, its representative lengths in charnockite and khondalite were taken for calculation of total length of lineament in different lithotypes. The calculated values of spatial index R and Z test (at the level of 5% significance) for each set of shear-lineaments are given in the table 2.

Conclusion

The following conclusions were drawn from the nearest-neighbor analysis for each set of lineaments of the study area.

The lineaments were evidently controlled by the geomorphological (lowlands and highlands) and lithological (khondalites and charnockites) factors. The division of the study area into two regimes, viz. TGS and ATS regimes, is justified by (i) the exclusiveness of some lineaments to certain regimes; for example NW-SE dextral major L2 lineaments confining to TGS regime (ii) variations of shear characteristics between the zones; for example NW-SE sinistral L3 of ATS regime of D3 deformation is observed only as sinistrally reactive L2 of TGS regime of D2 deformation. The nonsignificance Z values and the R values indicate that the L1 shear-lineaments are not of significant expression in any regimes of any lithology or of relief. The subsequent charnockitisation of earlier gneiss obliterated the evidences of L1 of D1. While meso lineaments (10<l>1 km) of L2 were traced both in TGS and ATS regimes with uniform regular pattern, the major lineaments (50<l>10 km) of L2 were observed in TGS regime only. The incipient charnockite associations along the L2 (NW-SE TGS, dextral) and L2R' (NE-SW sinistral) lineaments of D2 deformation (figures 1, 5) give support forthe first episodic initiation of cordierite bearing incipient charnockitisation of earlier gneisses

due to CO2 gas infiltration and dehydration occurred during the D2 deformation[33].

The association of regular pattern of major and meso L2 lineaments of D2 with southern massive charnockites and the random patterns of L2 with the khondalites emphasize a genetic link between the L2 lineaments and southern massive charnockites. The massive charnockitisation of khondalites and the alignment of some of the incipient charnockites were formed along the shear system of D2 deformation. The earlier workers were of the view on TGS was a sympathetic shear of ATS[34].

The present study indicates that the WNW-ESE to NW-SE trending ATS lineament (L3) has a sinistral sense of slip, while NNW-SSE to NW-SE striking TGS lineament (L2) shows a dextral sense of slip, indicating that they belonged to two different times of deformation and an overprinting of sinistral ATS zone on the earlier existed, dextral TGS zone[17]. The general regular pattern of major L3 ATS lineament (trending WNW-ESE to NW-SE) belonging to D3 deformation is due to the development of sinistral L3 (WNW-ESE trending principal displacement zone (PDZ)) and its complementary sinistral L3P NW-SE trending shear (ie. P shears) along the pre-existed dextral L2P (WNW-ESE trending P shears) and along L2 dextral main (NW-SE-PDZ) deformation respectively. This is the reason for better development of L3P (NW-SE trending) shear over the main L3 (WNW-SE trending), shear over the main L3 (WNW-ESE trending).

Another episode of incipent and massive charnockites seen along the directions of L3, L3R, L3R', L3P and L3T shear-lineaments of D3 indicate a second generation of charnockites due to variable amount of CO_2 gas seepage along the shears of D3 (ATS) deformation. Large scale conversion of gneisses into charnockites was formed between ATS and Palghat-Cauvery shear[35-37]. The random and regular patterned L4 (N-S Toranamalai sinistral) and L4R' (E-W dextral) shear-lineaments of D4 deformation were observed in the charnockite and khondalites of the study area respectively. Shear-lineaments of D4 displacing the earlier lineaments of D2 and D3 were observed and D4 deformation was initiated after the formation of incipent and massive charnockites of the study area.

Based on the lineament density and frequency distribution of patterns of observed shear-lineaments of the study area, the order of prominent shear-lineaments were (1) WNW-ESE to NW-SE sinistral, ductile deformation ATS lineaments and (2) NNW-SSE to NW-SE dextral, brittle dominant TGS lineaments which were affected the whole study area. The N-S sinistral, brittle Toranamalai shear-lineament comes third in the order and affected isolated areas only.

The development of all kinds of complementary shears of simple shear viz. Riedel R conjugate Riedel R', P shears symmetrical to R' shears and T-shears developed at an angle of 45° to PDZ (WNW-ESE) during the ductile-brittle ATS was due to high degree of intensity of D3. Sinistrally displaced quartzite exposure for 4 km is observed along Achankovil Shear zone near Tenkasi (figure 1). Based on the meanlinear density and mean frequency distribution of shear-lineaments of each deformation, the decreasing order of intensity of deformation was predicated as follows, ie. D3 ATS, D2 TGS, D4 Toranamalai shear and D1. The nearest neighbor analysis of shear-lineaments is a good tool to identify the order of intensity of deformations of the area. It is also possible to distinguish lineaments of different ages and inturn to differentiate the associated features and lithology of different ages.

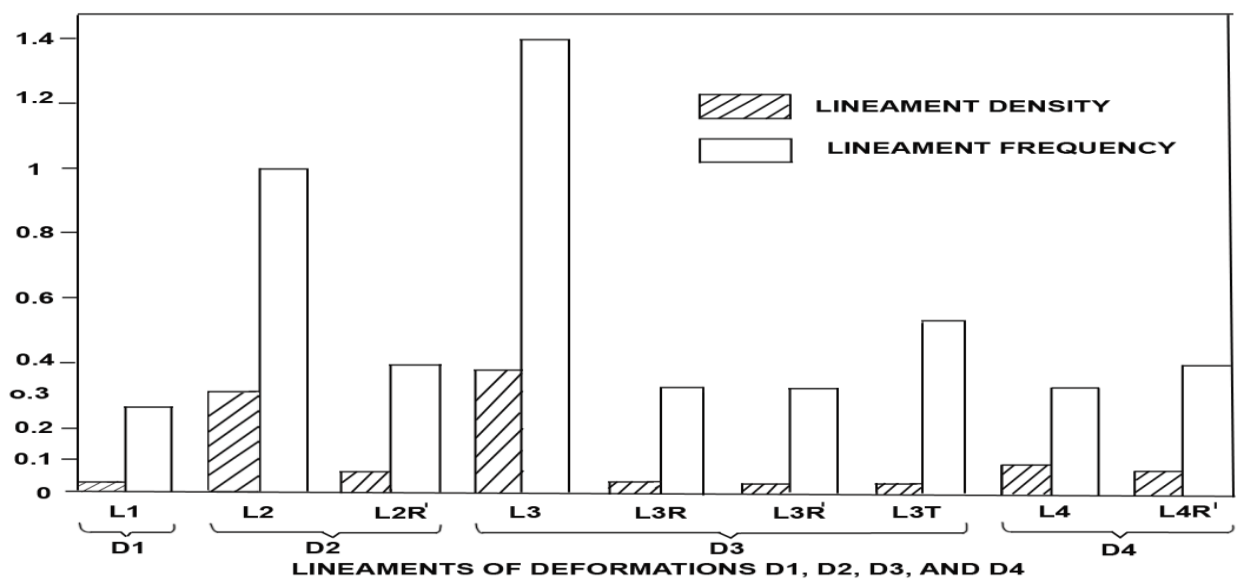

Figure-8
Density and frequency distribution of shear-lineaments of D1, D2, D3 and D4 deformation from Ambasamudram-Tenkasi transect

Table-2
The table reveals the values of spatial index R and Z test obtained from nearest-neighbor analysis of each set of shear-lineaments of D1, D2, D3 and D4 deformations for different regimes i.e. Shear lithology and geomorphology, ATS-Achankovil-Tambraparani shear; TGS-Tenmalai-Gatana shear. Spatial index R>2.15 imply regular pattern; S-significant regular pattern and NS-nonsignificant random pattern

	Shear Lineament index R & Z values	ATS Zone	TGS Zone	Total Highland regime	Total Low Land regime	Total Khondalite regime	Total Charnockite regime
D1	L1 Meso R	0.364	1.297	Nil	0.798	0.945	NS
	Z	-0.899NS	0.420 NS	Nil	-0.351NS	0.096 NS	NS
D2	Major R	Nil	2.890	0.997	0.842	1.056	0.571
	Z	Nil	4.225 S	-0.008 NS	-0.386NS	0.137 NS	-0.960 NS
	L2 R	0.347	1.000	0.519	0.171	0.794	0.628
	Meso Z	-2.519 S	-2.362 S	0.617 NS	-2.486 S	-0.545 NS	-0.910 NS
	L2R' Meso R	0.411	1.093	0.416	0.159	0.164	0.204
	Z	-2.505 S	-2.508 S	-2.545 S	-2.659 S	-3.827 S	-2.758 S
D3	Major R	2.14	1.663	-	-	-	-
	Z	3.016 S	0.938 NS	-	-	-	-
	L3 R	0.415	0.520	0.459	0.432	0.571	0.324
	Meso Z	-4.355 S	-2.293 S	-3.505 S	-1.703NS	-2.815 S	-2.242 S
	L3R Meso R	0.393	0.675	0.498	0.396	0.517	0.094
	Z	-1.639NS	-1.663 NS	-1.327NS	-2.005 S	-1.872 NS	-1.812 NS
	L3R' Meso R	0.319	0.485	0.583	0.202	0.292	0.365
	Z	-3.143 S	-1.655 NS	-1.319NS	-2.524 S	-2.651 S	-2.376 S
	L3T Meso R	1.104	Nil	0.366	0.070	0.223	0.192
	Z	-2.179 S	Nil	-1.678NS	-2.278 S	-2.198 S	-2.137 S
D4	L4 Meso R	0.926	1.497	0.197	0.489	0.301	1.040
	Z	-2.791 S	-2.339 S	-3.313 S	-1.694NS	-3.352 S	0.118 NS
	L4R' Meso R	0.790	0.457	0.674	0.256	0.201	0.486
	Z	-2.023 S	-2.605 S	-1.303NS	-2.105 S	-3.197 S	-1.453 NS

Acknowledgement

The first author thanks The Director, Institute of Remote Sensing, Anna University, Guindy, Chennai for extending the lab facilities. Our grateful thanks are due to Mr. A.P.C.V. Chockalingam, Secretary and Dr.C.Veerabhahu, Principal, V.O.Chidambaram College, Tuticorin for their encouragements, M.Ganapaty, Magy Arts Nellai and P.Neelamegam are duly acknowledged.

References

1. Ramsay J.G., Shear zones geometry: review, *J Struc Geol,* 83-99 **(1980)**
2. Ghosh S.K., Ductile Shear zones - A review of recent studies, *Q J Geol Miner, Soc India,* **57,** 183-202 **(1985)**
3. Ramsay J.G. and Huber M.I., *The techniques of modern structural geology,* **2,** Folds and Fractures, Academic press, New York, **(1987)**
4. Coward M.P., Shear Zones in the Precambrian crust of South Africa, *J Struc Geol,* **2,** 19-27 **(1980)**
5. Ramsay J.G. and Allison L., Structural analysis of shear zones in an Alpinised Hercinian Granite schweiz, *Miner Petrogr Mitt,* **59,** 251-279 **(1979)**
6. Simpson C. and Schmid S.M., An evaluation of criteria to deduce the sense of Movement in sheared rocks, *Bull Geol Soc America,* **94,** 1281-1288 **(1983)**
7. Cloos H., Experimenten zur inneren Tektonic. *Centralblatt fur mineralogic und Paleontologie,* 609 **(1928)**
8. Riedel W., Zur Mechanik geologischer Bruchersche-Inungen zentralblatt fur Mineralogie Geologie and Palaeontologie, Abhandlung B 354-368 **(1929)**
9. Tchalenko J.S., The evolution kink-bands and the development of compression texture in sheared clays, *Tectonophysics,* **6,** 159-174 **(1968)**
10. Mah A., Taylor G.R., Lennox P. and Balia L., Lineament analysis of Landsat Thematic Mapper Images, Northern Territory Australia, *Photogram Eng Remote Sens,* **61,** 761-773 **(1995)**
11. Rahiman T.I.H. and Pettinga J.R., Analysis of Lineaments and their relationship to Neogene fracturing, SE viti Levu Fiji, *Geol Soc Am Bull,* **20(11-12),** 1544-1555 **(2008)**
12. Kazemi R., Porhemmat J. and Kheirkhah M., Investigation of lineaments related to groundwater occurrence in a Karstic area: A case study in Lar catchment, Iran, *Res J Environ sci,* **3 (3)**, 367-375 **(2009)**

13. Guru Rajesh K. and Chetty T.R.K., Structure and tectonics of the Achankovil shear zone, Southern India, *Gonduwana Research,* **10,** 86-98 **(2006)**

14. Manimaran G., Three-Dimensional Finite Strain Patterns from Achankovil Transpression Zone, South India, *Outreach,* **2,** 70-75 **(2009)**

15. Manimaran D. and Manimaran G., Tectonics studies around Vallanadu area, Tuticorin District, TamilNadu, *Outreach,* **5,** 117-122 **(2012)**

16. Tapas Acharya, and Sukumar Basu Mallik, Analysis of lineament swarms in a precambrian metamorphic rocks in India, *J Earth System sci,* **121**(**2),** 453-462 **(2012)**

17. Manimaran G. and Roy Chacko P.T., Shear lineaments and tectonic setting of massive and incipient charnockites of Tambraparani shear zone, southern India, *International symposium on charnockite and granulite facies rocks, Aug 1996, held at Uni. of Madras, Madras, India, edited by Ram Mohan V.,* Abstract, 12-13 **(1996)**

18. Sacks P.E., Nambiar G.G. and Walters L.J., Dextral Pan African shear along the Southwestern edge of the Achankovil shear belt, south India: constraints on Gondwana reconstructions, *J Geol,* **105,** 275-284 **(1997)**

19. Rajesh H.M., Santosh M. and Yoshida M., Dextral Pan African shear along the Southwestern edge of the Achankovil shear Belt, South India, Constraints on gondwana reconstruction: A discussion, *J Geol,* **106,** 105-109 **(1998)**

20. Manimaran G., Deepak Bagai. and Roy Chacko P.T., Chrysoberyl from Southern TamilNadu of South TamilNadu, with implications for Gonduwana studies, *Mineral Exploration: Recent strategies, Eds, Rajendran S., et al. NewIndia Public Agency, NewDelh*i, 63-76 **(2007)**

21. Anderson E.M., *The dynamics of faulting,* **2,** Oliver and Boyd, Edinburgh, 206 **(1951)**

22. Skempton A.W., Some observations on tectonic shear zones, *First International Congress on Rock Mechanics, Proceedings,* **1,** 329-335 **(1966)**

23. Morgenstern N.R. and Tchalenko J.S., Microscopic structures in kaolin subjected to direct Shear, *Geotechnique,* **17,** 309-328 **(1967)**

24. Tchalenko J.S., Similarities between shear zones of different magnitudes, *Geological Society of America Bulletin,* **81,** 165-1640 **(1970)**

25. Tchalenko J.S. and Ambraseys N.N., Structural analysis of the Dasht-e-Bayaz (Iran) earthquake fracture, *Geol Soc Am Bull,* **81,** 41 **(1970)**

26. Wilcox R.E., Harding T.P. and Seely D.R., Basic wrench tectonics, *Amer Assoc Petrol Geol,* **57,** 74-96 **(1973)**

27. Bell T.H and Johnson S.E., Shear sense a new approach that resolves conflicts between criteria in metamorphic rocks, *J Metamorphic Geol,* **10(1),** 99-124 **(1992)**

28. Sylvester A.G., Strike-slip faults, *Geol Soc Amer Bull,* **100,** 1666-1703 **(1988)**

29. Naylor M.A., Mandl G. and Sijpesteijn C.H.K., Fault geometries in basement induced wrench faulting under different initial stress states, *J Struc Geol,* **8,** 737-752 **(1986)**

30. Ramsay J.G., *Folding and fracturing of rocks,* NewYork, McGraw Hill, 568 **(1967)**

31. Manimaran G., Petrological and structural studies of the North western part of the Tambraparni shear zone, South India, *Ph.D Thesis, Uni. of Kerala, Trivandrum, India, 289* **(1995)**

32. Davis J.C., *Statistics and data Analysis I Geology,* **2,** John Willey & sons, New York, 308-314 **(1986)**

33. Santosh M. and Drury S.A., Alkaligranites with Pan-African affinities from Kerala, South India, *J Geol,* **96,** 616-626 **(1988)**

34. Drury S.A., Harris N.B.W., Reeves Smith G.J. and Wightman R.T., Precambrian tectonics of crustal evolution in South India, *Journal of Geology,* **92,** 3-20 **(1984)**

35. Srikantappa C., Raith M. and Spiering B., Progreessive charnockitisation of leptynite khondalite suite in southern Kerala, India; Evidence for formation of charnockite through decrease in the fluid pressure, J *Geol Soc India,* **96,** 1-10 **(1985)**

36. Unnikrishnan Warrier C., Yoshida M., Kagami H. and Santosh M., Geochronological constraints on granulite formation is southern India, Implication for east Gondwana Reassembley, *Jou Geoscie Osaka city, Uni,* **36,** 109-121 **(1993)**

37. Jayananda M., Janardhan A.S., Sivasubramanian P. and Peucat J.J., Geochronologic isotopic constraints on granulite formation in the Kodaikanal area, South India and Antartic during the precambrian, *Mem Geol Soc India,* edited by Santosh M. and Yoshida M., **34**, 373-390 **(1995)**